Generative Adversarial Networks Applied to Synthetic Financial Scenarios Generation

Christophe GEISSLER*
Nicolas MORIZET*
Matteo RIZZATO*†
cgeissler@advestis.com
nmorizet@advestis.com
mrizzato@advestis.com
Advestis
Paris, France

Julien WALLART julien.wallart@fujitsu.com Fujitsu Systems Europe Labège, France

ABSTRACT

The finance industry is producing an increasing amount of datasets that investment professionals can consider to be influential on the price of financial assets. These datasets were initially mainly limited to exchange data, namely price, capitalization and volume. Their coverage has now considerably expanded to include, for example, macroeconomic data, supply and demand of commodities, balance sheet data and more recently extra-financial data such as ESG scores. This broadening of the factors retained as influential constitutes a serious challenge for statistical modeling. Indeed, the instability of the correlations between these factors makes it practically impossible to identify the joint laws needed to construct scenarios.

Fortunately, spectacular advances in Deep Learning field in recent years have given rise to GANs. GANs are a type of generative machine learning models that produce new data samples with the same characteristics as a training data distribution in an unsupervised way, avoiding data assumptions and human induced biases. In this work, we are exploring the use of GANs for synthetic financial scenarios generation.

This pilot study is the result of a collaboration between *Fujitsu* and *Advestis* and it will be followed by a thorough exploration of the use cases that can benefit from the proposed solution. We propose a GANs-based algorithm that allows the replication of multivariate data representing several properties (including, but not limited to, price, market capitalization, ESG score, controversy score, ...) of a set of stocks. This approach differs from examples in the financial literature, which are mainly focused on the reproduction of temporal asset price scenarios. We also propose several metrics to evaluate the quality of the data generated by the GANs. This approach is well fit for the generation of scenarios, the time direction simply arising as a subsequent (eventually conditioned) generation of data points drawn from the learned distribution.

Our method will allow to simulate high dimensional scenarios (compared to $\lesssim 10$ features currently employed in most recent use cases) where network complexity is reduced thanks to a wisely performed feature engineering and selection. Complete results will be presented in a forthcoming study.

KEYWORDS

Generative Adversarial Networks, Data Augmentation, Financial Scenarios, Risk Management

1 INTRODUCTION

1.1 General context

The investment industry has long been a major consumer of artificial data. An important application is the use of so-called Monte Carlo methods [7]: this can be used to price complex contracts for which no closed-form expression is available, or to estimate the risk of a portfolio by studying the statistical distribution of its possible values at a given horizon. In this framework, the main ingredient is a set of scenarios for the evolution of variables subject to randomness, including financial asset prices. Since Monte Carlo methods essentially proceed by averaging over a set of possible scenarios, this set must possess at least two statistical properties: i) the scenarios must be sufficiently numerous and constitute a representative set of all possibilities, ii) their trajectories must be individually compatible with a consensus model. When a stochastic model describing the evolution of the data is available, the task of generating scenarios is reduced to sampling from a multivariate distribution whose law is known. This approach makes it possible, for example, to model low-dimensional multivariate Gaussian distributions, assuming constant or deterministic covariances. Unfortunately, this situation is too simplistic for the needs of an asset portfolio manager, for the following reasons: i) the joint laws of the assets are not known with sufficient precision, ii) these joint laws are in general not stationary. In addition, an asset manager must be able to produce scenarios conditional on macroeconomic assumptions provided by the financial regulator, or by an internal economic research department. Models such as the Black-Litterman model [3] allow for the incorporation of a priori assumptions on future asset returns when these follow a known law. However, to our knowledge, there is no analytical framework that allows multidimensional asset returns to be conditioned on scenarios involving global variables correlated with these assets, such as inflation, oil prices or interest rates. The general mechanism of GANs makes it possible, as shown in this study, to fill this gap.

^{*}The authors are listed in alphabetic order.

[†]Corresponding author.

1.2 Previous work

In this section we review previous works which focus on the generation of financial market scenarios highlighting the conceptual innovation of our study. Mainly, rather than learning temporal patterns, we aim to catch instantaneous correlations among mediumlong horizon asset returns and macroeconomic variables, their joint distribution being assumed almost stationary over several units of time (each unit of time corresponds to a market realization, which can be daily, monthly, ...). Such innovative perspective has also an impact at the level of models' architecture. In particular, recurrent networks can be dropped in favor of much lighter structures, such as simple multi-layer perceptrons (MLP), which are furthermore capable to deal with higher dimensional data sets (typical investment portfolios may include up to several tens of lines).

Neural Network-based generative techniques have been applied only recently to the domain of financial time series, the earliest works being published in late 2018. In [25], the authors employed a LSTM-based GANs to mimic a 20 years historical period for 2 financial indices and 3 individual stocks' prices. In 2019 [19] FIN-GAN was introduced as a deep neural network-based GAN, its performance being evaluated on the generation of a synthetic S&P500 index. In [23] the authors propose TimeGAN, a generative framework capable to preserve the temporal dynamics of multi-dimensional time series in terms of the probability of a newly generated point conditioned on the value of previously generated one. Its performance is evaluated in terms of diversity, fidelity and via the well known criterion train-on-synthetic, test-on-real on 6-dimensional Google stocks data from 2004 to 2019 (volume, high, low, opening, closing and adjusted closing). A generative framework always dedicated to time series is also proposed in [22]. In this last study, the authors employ Temporal convolution Networks [20] within the generator aiming at capturing long-range dependencies such as volatility clusters. The overall architecture is employed for the generation of a synthetic one-dimensional S&P 500 index. Finally, we mention the work presented in [13], as it is of particular relevance for our case study. As a matter of facts, i) the authors tackle the generation of a high number (~600) of assets' historical returns and ii) there is an explicit declaration of intent regarding the future use of their work for conditional generation in the context of strategies' stress tests. However, [13] is still far from our proposed framework: while it is true that conditioning is explicitly introduced (in fact, conditional GANs are employed), yet the conditioning is done over the past assets' values within a fixed time horizon. Differently said, reproducing short-time historical patterns is still the main concern. On top of that, the proposed studies only deals with one-dimensional time series whereas realistic strategies have an underlying investing universe of several hundreds of possible financial instruments, eventually correlated. Summing up, the work presented in [13] assumes that the temporal behavior of a single asset financial time-series can be predicted thanks to a memory effect over a fixed past horizon. This assumption is questionable and the absence of linear correlations is widely documented [5]. As previously declared, we aim at learning/reproducing the joint probability of medium-horizon returns (~ monthly) and slow varying environmental variables guiding the medium-long term market behavior.

2 GENERATIVE ADVERSARIAL NETWORKS

Introduced in 2014, by Ian Goodfellow et al. [8] to circumvent the intractability of probabilistic computations encountered by Deep Generative models during maximum likelihood estimation, Generative Adversarial Networks (GANs) have shown groundbreaking results in image generation. Since their creation they have been adapted to a broader range of applications from speech synthesis (Bińkowski et al. [2]) to gravitational burst generation (McGinn et al. [14]) or even dynamic environments simulation (Kim et al. [12]).

In this work, we will benefit from the coupled use of two types of GANs architecture, this partition mirroring a physically-motivated assumption regarding macro-economic state variables driving the time evolution of instrument-specif properties over time. The first model is a Bidirectional GANs (BiGAN) and it is dedicated to the generation of state variables, eventually conditioned on macro-economic scenarios. The second model is instead a Conditional GANs which is deployed for the recurrent generation of different instrument features evolution over time. The output of the former will condition the output from the latter. We defer to App. B an in depth technical analysis of the GANs tecnology.

3 ECONOMIC SCENARIO GENERATION

3.1 Historical dataset

Let us formalise the content presented in Sec. 1. We consider a tabular set of historical data $\{y_i\}_{i=1,\dots,n}$. Each sample is composed of n^i instrument-specific features, the respective n^i transitions $t \to t+1$ and n^s state variable transitions. The possibility to describe financial time series via tabular data lies on the assumption of them being Markovian series. In particular, a single sample y_i is structured as follows

$$\mathbf{y}_{i_{k,t}} = \{ \mathbf{i}_t^{\mathbf{k}}, \Delta \mathbf{i}_t^{\mathbf{k}}, \Delta \mathbf{s}_t \} \tag{1}$$

where

 $\emph{\textbf{i}}_t^k$ is the vector of the features univocally characterising the instrument k at time t,

 Δi_t^k is the vector of transition $t \to t+1$ for the features i^k Δs_t is the value for the transition $t \to t+1$ for a chosen set of meaningful macro-economic variables

In the training set, Δi_t^k can be obtained from i_t^k and i_{t+1}^k via any user-specified function¹. In general, we note \star the following operator

$$\mathbf{i}_{t+1}^{\mathbf{k}} = \mathbf{i}_{t}^{\mathbf{k}} \star \Delta \mathbf{i}_{t}^{\mathbf{k}}. \tag{2}$$

In Eq. (1) we did not include the values of the state variables at time t, which we eventually note as s_t . This strongly depends on the model choices: state variable transitions are completely decorrelated from their levels. Any different assumption will require the features s_t to be included in the historical dataset along with those listed in Eq. (1). Let us underline that the depth of the user-provided transitions Δi_t^k automatically sets the maximum resolution of the future simulation: one month variations, for example, allows for a simulation of minimum step of one month.

 $^{^{1}\}mathrm{For}$ example, it may be relative return for prices or absolute variations for correlations.

3.2 Training procedure

Starting from the historical dataset

$$\mathcal{D}_{\mathcal{H}} = \left\{ \mathbf{y}_{i_{k,t}} \right\}_{k=1,\dots,K}^{t=1,\dots,T}, \tag{3}$$

two training datasets are built, each being used for a specific GANs architecture.

The first dataset $\mathcal{D}_{\mathcal{S}}$ is used to train a BiGAN-type architecture $\{\mathcal{S},\mathcal{Z}\}$ dedicated to i) respectively sample from the joint distribution of the state variable transitions and to ii) inverse map \mathcal{P}_s such variations back into the original latent space

Training
$$\mathcal{D}_{\mathcal{S}}: \{\Delta \mathbf{s}_t\}_{t=1,\dots,T} \quad \mathbf{z}^{\mathbf{s}} \sim \left[\mathcal{N}_{0,1}\right]^{\ell_{\mathbf{s}}}(\mathbf{z})$$

Inference $\hat{\Delta \mathbf{s}} = \mathcal{S}(\hat{\mathbf{z}}^{\mathbf{s}}), \quad \hat{\mathbf{z}}^{\hat{\mathbf{s}}} = \mathcal{Z}(\Delta \mathbf{s}), \quad \hat{\Delta \mathbf{s}} \stackrel{\mathcal{S}}{\sim} \mathcal{P}_{\mathbf{s}}(\Delta \mathbf{s})$

A second dataset $\mathcal{D}_{\mathcal{E}}$ accounts for the time-dependent information and it is used to train a second GANs architecture \mathcal{E} . This second network learns to sample future transitions $\Delta \mathbf{i}_t^k$ of the instrument-specific features, conditioned on a vector of state variable transitions $\Delta \mathbf{s}_t$ and the current instrument state \mathbf{i}_t^k

$$\begin{array}{ll} \text{Training} & \mathcal{D}_{\mathcal{E}} \; : \; \left\{ \{i_t^k, \Delta \mathbf{i}_t^k, \Delta \mathbf{s}_t\} \right\}_{\substack{t=1,\ldots,t\\k=1,\ldots,K}}, \quad \mathbf{z^e} \sim \left[\mathcal{N}_{0,1}\right]^{l_i}(\mathbf{z}) \\ \text{Inference} & \Delta \mathbf{i} = \mathcal{E}\left(\mathbf{z^i}; \mathbf{i}, \Delta \mathbf{s}\right), \quad \Delta \mathbf{i} \sim \mathcal{P}_{\mathbf{i}}\left(\Delta \mathbf{i}; \mathbf{i}, \Delta \mathbf{s}\right) \end{array}$$

3.3 Market scenarios and conditioned generation

As we saw in Sec. 3.2, the generator S learns to draw samples from the joint distribution \mathcal{P}_s (Δs). However, it is important for the case study of interest to generate samples, at time t, assuming an underlying macro-economic scenario of interest when transitioning from realisations at time t to t + 1. Formally, this is realised by conditioning the generation within an hyper-rectangular condition $\Delta s_t \in I_t$. Conditional GANs do already exists [15]: however, these algorithms are note suited for our case study as market conditions are described by continuous values which are not known a priori. For this task, we rather exploit the condition-agnostics generator ${\cal S}$ via a Bayesian approach. If we explicitly knew the learnt distribution \mathcal{P}_{s} (Δs) (likelihood), then we could use Markov Chain Monte Carlo (MCMC) techniques to sample Δs from the product (posterior) $\mathcal{F}(\Delta s; I_t) = \mathcal{P}_s(\Delta s) \cdot \mathcal{W}_{I_t}(\Delta s)$ between \mathcal{P}_s and a window function $\mathcal{W}_{I_{r}}\left(\Delta s\right)$ (prior) designed to be 1 for Δs \in I_{t} and 0 elsewhere. Unfortunately, the generator S only learns an implicit distribution.

However, it does learn a non-linear mapping $z^s \xrightarrow{S} \Delta s$ where z^s is drawn from an analytical distribution $[\mathcal{N}_{0,1}]^{l_s}(z)$. It can be proven [17] that samples drawn via the following process

$$\{\Delta \mathbf{s}\} \stackrel{\text{MCMC}}{\sim} \mathcal{F}(\Delta \mathbf{s}; \mathbf{I}_t)$$
 (4)

have the same statistical properties as if obtained via

$$\{\Delta \mathbf{s}\} \overset{\mathcal{S}}{\leftarrow} \{z^{\mathbf{s}}\}$$

$$\{z^{\mathbf{s}}\} \overset{\mathrm{MCMC}}{\sim} \left[\mathcal{N}_{0,1}\right]^{l_{\mathbf{s}}} (z) \cdot \mathcal{W}_{\mathbf{I}_{t}} (\mathcal{S}(z)) . \quad (5)$$

The method proposed in Eq. (5) is then used to sample state variable transitions including a-priori assumption on the underlying economic scenario. A suitable starting point \hat{z}^s for the MCMC can be identified thanks to the encoder \mathcal{Z} by inverse-mapping a variation $\hat{\Delta s}$ which we know satisfies the scenario, i.e. $z_0^s = \mathcal{Z}(\Delta s_0)$ with $\hat{\Delta s} \in I_t$.

3.4 Trajectories construction

Single instrument trajectory. The algorithmic unity of the proposed simulator is the generation of instrument-specific features i_{t+1}^k starting from the previous state i_t^k and conditioned on a user-determined scenario I_t . A trajectory \mathcal{T}^k of historical depth p for the k^{th} instrument is obtained by generating p instrument levels $\{i_0^k, i_1^k, \ldots, i_t^k\}$, each one conditioned on the previous one and on the market context. Algorithm 1 allows the regressive generation of \mathcal{T}^k starting from user-specified initial conditions i_0^k and scenarios $\{I_0, \ldots, I_{p-1}\}$.

Algorithm 1 Single trajectory generation for the k^{th} instrument

Require:
$$i_0^k$$
, $\{I_0, \dots, I_{p-1}\}$
 $t = 0$
while $t \leq p$ do
$$\Delta s \overset{\text{MCMC}}{\sim} \mathcal{F}(\Delta s; I_t)$$
 $z \sim \left[\mathcal{N}_{0,1}\right]^{l_s}(z)$

$$\Delta i \leftarrow \mathcal{E}\left(z; i_t^k, \Delta s\right)$$
 $i_{t+1}^k \leftarrow i_t^k \star \Delta i$
end while

Please note that it is possible to simulate the behaviour of a real financial instrument by mapping its features into the corresponding context i_0^k .

Portfolio trajectory. Our ultimate goal is to thoroughly describe the statistical properties of a portfolio including K instruments at different time steps. For this purpose, n_t , $n_t \lim \to \infty$ trajectories must be generated for each instrument k so to obtain an unbiased reconstruction of the feature distributions $\left\{\mathcal{P}_i\left(\Delta i;i_t^k,I_t\right)\right\}_{t=1,\dots,p}$. Further, it is desirable to combine instrument-level features to obtain portfolio-level features, along with their statistical properties. Building upon Algorithm 1, in Algorithm 2 we outline the whole portfolio simulation procedure. In Appendix A we prove that the samples $\{\Delta i_{t,1}^k,\dots,\Delta i_{t,n_t}^k\}$ can be used to build histograms which are unbiased estimators of the marginal distributions for each of the feature components at time t. More formally (for simplicity we drop the labels k and t), for the c^{th} feature (c^{th} component of i) conditioned on a past state \hat{a} and a scenario I, we prove that the mean number count $\hat{\mathbb{B}}_c^{[-,+]}$ within the bin of limits [+,-]

$$\hat{\mathbb{B}}_{c}^{[-,+]} \equiv \frac{1}{n_{t}} \sum_{j=1}^{t} \Theta_{-}^{+}(\Delta i_{c,j}),$$

$$\Theta_{-}^{+}(e) = \begin{cases} 1, & \text{if } e \in [-,+], \\ 0, & \text{else} \end{cases}$$
(6)

Algorithm 2 Portfolio simulation

```
Require: \{i_0^k\}_{k=1,...,K}, \{I_0,...,I_{p-1}\}, I_t \times S_t = n_t for unique I_i \in \{I_0,...,I_{p-1}\} do

S_i \equiv \{\Delta s_j\}_{j=1,...,S_t}; \quad \Delta s_j \stackrel{\text{MCMC}}{\sim} \mathcal{F}(\Delta s; I_i) end for t=0
while t \leq p do

Z = \{z_i\}_{i=1,...,I_t}; \quad z_i \sim \left[\mathcal{N}_{0,1}\right]^{l_e}(z)
ZS_t = Z \times S_t
while k \leq K do
while m \leq n_t do
\{z, \Delta s\} \stackrel{\text{no repl.}}{\sim} ZS
\Delta i \leftarrow \mathcal{E}(z; i_{t,m}^k, \Delta s)
i_{t+1,m}^k \leftarrow i_{t,m}^k \star \Delta i
end while
end while
end while
```

is an unbiased estimator for the true binned marginal distribution

$$\begin{split} \mathbb{B}_{c}^{\left[-,+\right]} &\equiv \int_{-}^{+} \mathrm{d}\Delta i_{c} \, \mathcal{P}_{m} \left(\Delta i_{c}; \hat{\boldsymbol{a}}, I\right), \\ \mathcal{P}_{m} \left(\Delta i_{c}; \hat{\boldsymbol{a}}, I\right) &= \int \prod_{\hat{c} \neq c}^{n^{i}} \mathrm{d}\Delta i_{\hat{c}} \, \mathcal{P}_{i} \left(\Delta i; \hat{\boldsymbol{a}}, I\right) \end{split} \tag{7}$$

Step by step, in Algorithm 2 a user must specify a context (initial conditions) for each of the instrument in the portfolio, i.e. $\{i_0^k\}_{k=1,\dots,K}$. At each time step, the total number of trajectories n_t is achieved by combining two possible sources of randomness: S_t samples obtained via the Bayesian procedure explained in Sec. 3.3 combined with I_t samples from the second latent space. In order to grasp the intra-portfolio correlations, these samples are kept fixed for all the instruments at a given time. As some of the market scenarios may be repeated during the simulation, we advise to MCMC-sample the state variable transitions only once per unique scenarios (first loop in Algorithm 2). At time t, the sampled state transitions S_t are then combined via a simple Cartesian product with a bunch of points Z in second generator's latent space. When iterating over trajectories, the algorithm will uniformally sample (with no replacement) from the Cartesian product ZS_t .

4 DATASET

4.1 Data Selection

For this proof of concept, we focus on equities as financial instruments. We have chosen data that are at the same time very heterogeneous in their statistical distributions, and at least intermittently influential on the dynamics of stock prices. As explained in Sec. 3, the variables are divided into specific variables and state (or global) variables. Specific variables are attributes specific to each stock, which will influence the marginal behavior of the price of that stock in relation to the average. State variables correspond to macroeconomic quantities that can affect the movement of stocks as a whole. By combining these two types of variables, it is therefore

possible to account for the movements of the average stock ("the market"), as well as the relative movements of stocks with respect to the market.

The specific variables, defined for each stock, are:

- The daily closing price adjusted for dividends.
- The market capitalization.
- Overall ESG score.
- Level of controversy.
- 1-year rolling correlations of daily returns with those of Energy, Consumer Staples, Financials and Information Technology sectors.
- Normalized trend over the past month and 12 months.
- 1-year rolling volatility.

The choice of these specific variables is supposed to constitute the time-dependent "identity card" of an issuer. These variables are supposed to allow a differentiation of the price behavior of issuers when they are subjected to the same variations of the market environment represented by the state variables.

The state variables are:

- The general level of the stock markets, represented by the S&P 500 index.
- The risk level of the equity markets, represented by the VIX index.
- The slope of the EUR yield curve, represented by the spread between 1-year and 10-year swap rates.
- The price of a barrel of WTI oil.
- The EUR/USD exchange rate.
- The premium of the Italian credit default swap.
- The price of an ounce of gold in USD.

4.2 Data Collection

The data used in our experiments come from two providers: $Capital\ IQ^2$ for the financial data (such as prices and market capitalizations) and $Vigeo\ Eiris^3$ regarding the extra-financial data (such as ESG and controversy scores). The historical depth of the data is almost 10 years (from 2011/09/30 to 2021/04/22). Those data are divided into two groups: equity (specific) variables (EQV) and state (global) variables (STV), details being depicted in Tab. 2 and Tab. 3, respectively.

4.3 Data Preparation

Some basic data processing techniques are applied to variables. First, every missing values due to non-availability of data at every business day (e.g monthly or quarterly data), are filled forward using the latest known value.

Some variables are subject to affine normalization, in order to rescale them into [0, 100].

²Capital IQ website: https://www.capitaliq.com

³Vigeo Eiris website: https://vigeo-eiris.com

4.4 Feature Engineering

This step is essential in the constitution of the dataset.

For each variable $V_i=EQV_i$ or $V_i=STV_i$, forward-looking transitions (absolute or relative) are calculated: the absolute transition is defined by $\Delta_{\rm abs}^{i,t}=V_i(t+\Delta t)-V_i(t)$ whereas the relative transition is computed as $\Delta_{\rm rel}^{i,t}=\frac{V_i(t+\Delta t)}{V_i(t)}-1$, where Δt is the time step (here, $\Delta t=1$ month or 20 rows of data). For features representing a price or an accreted return, and that must keep positive values in any case, the relative transition is used. For other features, in particular those taking positive or negative values, the absolute transition is used.

The rationale behind it is to teach GANs the implicit correlations between transitions in macroeconomic variables, and changes in stock-specific variables, in particular the stock price. The knowledge of the transitions of the specific variables allows by recurrence to generate the state in t + H from the state in t. The counterpart of this method is that the GAN is specifically trained to model transitions for a certain horizon H (H = 1 month or 20 business days in our case). The generation of trajectories over longer durations is simply done by concatenating elementary trajectories of duration H

4.5 Final dataset

For this experiment, we have deliberately removed the levels of state variables from the dataset, only keeping their transitions. This allows the GAN not to be over-influenced by the particular chronology of state variables, and not to infer spurious generalities from the time elapsed by the gold price around 1000 USD an ounce, for example.

We thus have the following sequence for the features (Tab. 1):

Table 1: Order of the features: the first 11 EQV values followed by the 11 corresponding EQV transitions, then the 7 STV transitions.

$$EQV_{i=1...11}$$
 $\Delta_{EQV_{i=1...11}}$ $\Delta_{STV_{i=1...7}}$

The dataset is composed of 10 batches of 10,000 two-dimensional layers of size $s_l = (n_s \times n_f)$, built at a random date, where n_s is the number of randomly chosen stocks among a total of 324 and n_f the number of common features (equity and state variables). Constructing each layer is a challenging task since the data are very sparse. A thorough checking procedure is performed to ensure that each layer is fully populated thus the GANs can learn correctly. After stacking all the layers together and reshaping the data, we obtain a matrix of size ([100,000 $\times n_s$] $\times n_f$). In our study, n_s = 10 and n_f = 29, thus leading to a matrix M of size (1,000,000 \times 29).

5 ARCHITECTURE

In this section, we present the architectures we deployed for this first pilot study. In an upcoming analysis, we will optimize the networks according to the performance metrics we introduce in Sec. 6.

Table 2: The 11 Equity variables (EQV).

Feature	Meaning	Transition
$\overline{EQV_1}$	Price	Relative
EQV_2	Market cap (in €B)	Relative
EQV_3	ESG score	Absolute
EQV_4	Controversy score	Absolute
EQV_5	Consumer staples sector correlation	Absolute
EQV_6	Energy sector correlation	Absolute
EQV_7	Financials sector correlation	Absolute
EQV_8	IT sector correlation	Absolute
EQV_9	Normalized price variation over 1 month	Absolute
EQV_{10}	Normalized price variation over 1 year	Absolute
EQV_{11}	Annualized volatility over 1 year	Absolute

Table 3: The 7 State variables (STV).

Feature	Meaning	Transition
STV1	Level of the equity market (S&P 500)	Relative
STV2	Risk level of the equity market (VIX)	Absolute
STV3	Spread between 1-year and 10-year interest rate swaps (in EUR)	Absolute
STV4	WTI crude price (in USD)	Relative
STV5	EURUSD exchange rate	Relative
STV6	Proxy of insolvency risk for Italy	Absolute
STV7	Gold price per ounce (in USD)	Relative

5.1 Bidirectional GANs (S, \mathbb{Z})

The reference networks retained for the BiGAN architecture are described in Tables 4, 5, and 6.

Table 4: Generator S

Layer	Norm./Act.	Output shape
Latent vector	-	8 x 1
ConvTranspose1D	BatchNorm / ReLU	256 x 3
ConvTranspose1D	BatchNorm / ReLU	128 x 5
ConvTranspose1D	BatchNorm / ReLU	64 x 7
ConvTranspose1D	- / Linear	1 x 7

Table 5: Discriminator

Layer	Norm./Act.	Output shape
Input / Latent	-	1 x 7, 8 x 1
Conv1D, Linear	SpectralNorm / LeakyReLU	64 x 5, 64 x 1
Conv1D, Linear	SpectralNorm / LeakyReLU	128 x 3, 128 x 1
Conv1D, Linear	SpectralNorm / LeakyReLU	256 x 2, 256 x 1
Conv1D, Identity	SpectralNorm / LeakyReLU	256 x 1, 256 x 1
Concat	-	512 x 1
Linear	SpectralNorm / LeakyReLU	256 x 1
Linear	SpectralNorm / Linear	1 x 1

Table 6: Encoder $\mathcal Z$

Layer	Norm./Act.	Output shape
Input	-	1 x 7
Conv1D	BatchNorm / LeakyReLU	64 x 5
Conv1D	BatchNorm / LeakyReLU	128 x 3
Conv1D	BatchNorm / LeakyReLU	256 x 2
Conv1D	BatchNorm / LeakyReLU	256 x 1
Linear	- / Linear	8 x 1

Generator latent variables are sampled from $\mathcal{N}(0,1)$. Spectral normalization layers [24] are added in discriminator while generator structure is left unchanged. Spectral normalization was in the first place proposed to increase generalization capabilities of Deep Learning models, reducing sensitivity to perturbation in input data. Later works [16] show that spectral normalization could be successfully used on GANs as another way to enforce a Lipschitz constraint on the discriminator. This weight normalization technique is applied on each layer at discriminator level thus no additional forward and backward pass is required to compute a gradient penalty term which is an interesting property to speed-up training phase. Also, as stated in [16], we used Hinge loss as these architectures perform better with this objective function.

$$\mathcal{L}_{D} = \mathbb{E}_{\mathbf{x} \sim p_{data(\mathbf{x})}} \left[min(0, -1 + D(\mathbf{x})) \right] - \mathbb{E}_{\mathbf{z} \sim p_{\mathbf{z}}} \left[min(0, -1 - D(G(\mathbf{z}))) \right]$$
(8)

$$\mathcal{L}_{G} = -\mathbb{E}_{\mathbf{z} \sim p_{\mathbf{z}}}[D(G(\mathbf{z}))] \tag{9}$$

5.2 Conditional GANs

The reference networks retained for the conditional GANs architecture are described in Tab. 7 and in Tab. 8.

Table 7: Conditional Generator $\mathcal E$

Layer	Norm./Act.	Output shape
Latent / Condition	-	8 x 1, 1 x 18
Linear	- / ReLU	8 x 1, 8 x 1
Concat	-	16 x 1
ConvTranspose1D	BatchNorm / ReLU	512 x 3
ConvTranspose1D	BatchNorm / ReLU	256 x 5
ConvTranspose1D	BatchNorm / ReLU	128 x 9
ConvTranspose1D	BatchNorm / ReLU	64 x 10
Linear	- / Linear	1 x 10

Table 8: Conditional Discriminator

Layer	Norm./Act.	Output shape
Latent / Condition	-	1 x 10, 1 x 18
Linear	- / ReLU	1 x 10, 1 x 10
Concat	-	2 x 10
Conv1D	SpectralNorm / LeakyReLU	64 x 10
Conv1D	SpectralNorm / LeakyReLU	128 x 5
Conv1D	SpectralNorm / LeakyReLU	256 x 3
Conv1D	SpectralNorm / LeakyReLU	512 x 3
Conv1D	SpectralNorm / Linear	1 x 1

6 PERFORMANCE EVALUATION

As we are not dealing with imagery databases, we have to design evaluation metrics that are relevant to tabular data, thus different from the ones used for images (such as the Fréchet Inception Distance [10], the Inspection Score [18] and the Neuroscore [21]). The quality of the generation is first evaluated at the level of the marginal distributions via a statistical metric, namely the *KS-score*. Secondly, we perform a first effort in trying to assess the generated joint distribution via the *Dimension reduction score* and the visual inspection of a triangle plot, an example being given in Fig. 1.

• KS score – The two-sample Kolmogorov-Smirnov test (KS test) [11] is used to verify whether two 1D samples come from the same distribution. This metric compares the distributions of continuous features using the empirical cumulative distribution function (CDF). For each feature, the similarity score is computed as one minus the KS test D-statistic, which indicates the maximum distance between the real data CDF (CDF_{real}) and the generated data CDF (CDF_{gen}) values. The output score S_{ks} lies in [0,1] and is computed as the mean score across all the features:

$$S_{ks} = \frac{1}{n_f} \sum_{i=1}^{n_f} (1 - \sup_{x_i} |CDF_{\text{real}}(x_i) - CDF_{\text{gen}}(x_i)|)$$
 (10)

 Dimension reduction score – A Principal Components Analysis (PCA) is performed on correlation matrices among features. The absolute relative error between the eigenvalues of the real dataset {e_i} and the eigenvalues of the generated dataset {ê_i} is used to obtain the dimension reduction score as follows:

$$S_{\text{pca}} = 1 - \frac{1}{N} \sum_{i=1}^{N} \min\left(1, \frac{|e_i - \hat{e}_i|}{e_i}\right)$$
 (11)

where N is the total number of eigenvectors kept during the reduction dimension process. In our experiments, the value of N is automatically chosen such that 99% of the variance is explained. Also, the relative errors are clipped in order to have the final score S_{pca} in [0, 1].

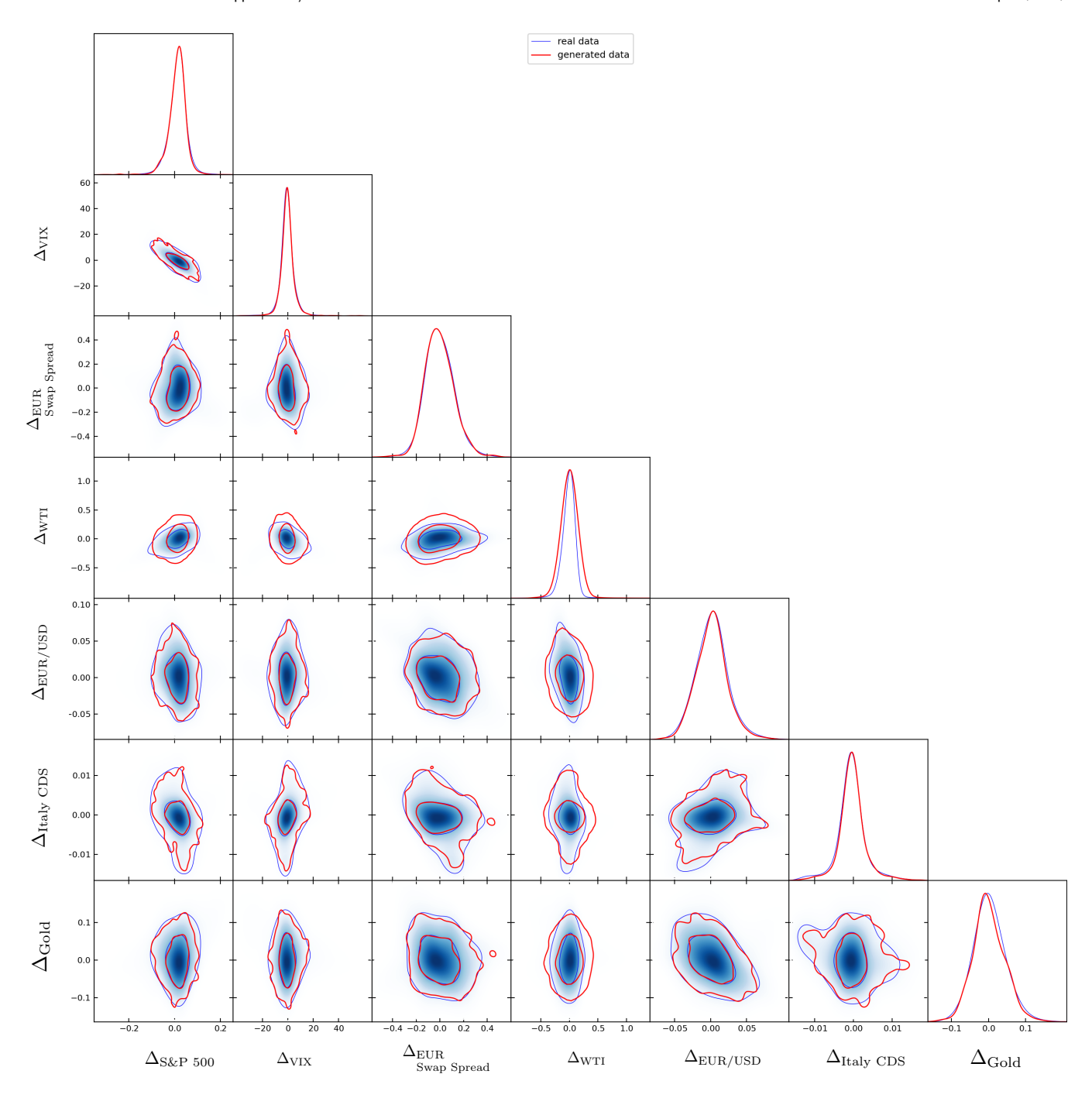


Figure 1: Example of Triangle plot. Comparison between the real (*blue*) and generated (*red*) state variable transitions. This visualization allows to compare one-dimensional (*diagonal panels*) and two-dimensional marginal distributions (*off-diagonal panels*) sorting them by couples of state variables. In each subplot, the 68% and the 95% confidence intervals are proposed.

7 DISCUSSION AND FUTURE WORK

7.1 Main results

We have presented here a GANs-based algorithm to reproduce economic contexts characterized by global observable variables and specific variables for financial assets. The methodology is used to generate, on fixed time steps, transitions of variables whose joint distribution is identical to the empirical distribution observed in the training set. We have therefore adopted a Markovian framework, in which the distribution of transitions on the stocks' specific variables

- in particular the price - is supposed to only depend on the state of observable variables (global or asset-specific) at the previous time. For this reason, the multi-layer neural nets used both for the generator and the discriminator is purely feed-forward and do not need to embed any time recurrence.

The first proof of validity of the proposed architecture consists in comparing the historical and artificial distributions of the variables. We propose statistical comparison metrics to evaluate not only the replication quality of mono-variate, but also of bi-variate distributions.

One of the main contributions of this pilot study is therefore the technical framework to generate random transitions on the specific variables of the assets, notably their price, which respects the historical correlation structure between these transitions, and the transitions of the other observable variables, such as the global variables. The unconditional generation of price trajectories over long horizons is then simply obtained by concatenating random trajectories conditioned on different time steps. To the best of our knowledge, this ability to generate multivariate trajectories independent of a stochastic model has not yet been presented in the financial literature.

Beyond the unconditional generation of trajectories, one interesting benefit of this architecture is the ability to condition trajectories to particular scenarios on one or several state variables. This ability stems directly from the two-way correspondence between the latent space and the real space of variables offered by the BiGAN structure, together with the use of a suitably adapted MCMC procedure. Both ingredients have been presented in the current paper. Practical applications of this principle will be illustrated in greater detail in a forthcoming paper.

7.2 Future work

While the purpose of the this first paper is to set up the technical environment of our solution, we plan further thorough explorations of the use cases that can benefit from the results here presented.

From a machine learning perspective, the determination of the optimal architectures for the different networks is highly experimental matter. Thanks to the performance metrics introduced in Sec. 6 it will be possible to tune them in a systematic matter ensuring high reproducibility of the historical data properties.

From a financial practitioner's point of view, the choice of the input variables is closely linked to the size of the time step used to model transitions. In this study, a one month time-step was used. This scale of variation is compatible with slowly varying input variables, like long-range correlations and volatilities, and ESG metrics. Should one decide to replicate daily price movements instead of monthly ones, another set of variables would have to be determined. More generally, an interesting research route is the setting of a scoring method giving for each variable a measure of how influential it is on the conditioning of future price transitions.

In order to fully prove its efficiency, this architecture will have to be declined on various datasets and time horizons, with a deterministic design procedure for the GANs architecture as a function of the datasets characteristics.

REFERENCES

- Martin Arjovsky, Soumith Chintala, and Léon Bottou. 2017. Wasserstein GAN. arXiv e-prints, Article arXiv:1701.07875 (Jan. 2017), arXiv:1701.07875 pages. arXiv:1701.07875 [stat.ML]
- [2] Mikolaj Bińkowski, Jeff Donahue, Sander Dieleman, Aidan Clark, Erich Elsen, Norman Casagrande, Luis C. Cobo, and Karen Simonyan. 2019. High Fidelity Speech Synthesis with Adversarial Networks. arXiv e-prints, Article arXiv:1909.11646 (Sept. 2019), arXiv:1909.11646 pages. arXiv:1909.11646 [cs.SD]
- [3] Fisher. Black and Robert Litterman. 1991. Asset Allocation Combining Investor View With Market Equilibrium. Journal of Fixed Income Vol. 1 No. 2 (Sept. 1991), pp. 7–18
- [4] Fabio Carrara, Giuseppe Amato, Luca Brombin, Fabrizio Falchi, and Claudio Gennaro. 2020. Combining GANs and AutoEncoders for Efficient Anomaly Detection. arXiv e-prints, Article arXiv:2011.08102 (Nov. 2020), arXiv:2011.08102 pages. arXiv:2011.08102 [cs.CV]
- [5] Rama Cont. 2001. Empirical properties of asset returns: stylized facts and statistical issues. Quantitative Finance 1 (2001), 223 – 236.
- [6] Jeff Donahue, Philipp Krähenbühl, and Trevor Darrell. 2016. Adversarial Feature Learning. https://doi.org/10.48550/ARXIV.1605.09782
- [7] Paul Glassermann. 2003. Monte Carlo methods in financial engineering.
- [8] Ian J. Goodfellow, Jean Pouget-Abadie, Mehdi Mirza, Bing Xu, David Warde-Farley, Sherjil Ozair, Aaron Courville, and Yoshua Bengio. 2014. Generative Adversarial Networks. arXiv e-prints, Article arXiv:1406.2661 (June 2014), arXiv:1406.2661 pages. arXiv:1406.2661 [stat.ML]
- [9] Ishaan Gulrajani, Faruk Ahmed, Martin Arjovsky, Vincent Dumoulin, and Aaron Courville. 2017. Improved Training of Wasserstein GANs. arXiv e-prints, Article arXiv:1704.00028 (March 2017), arXiv:1704.00028 pages. arXiv:1704.00028 [cs.LG]
- [10] Martin Heusel, Hubert Ramsauer, Thomas Unterthiner, Bernhard Nessler, and Sepp Hochreiter. 2018. GANs Trained by a Two Time-Scale Update Rule Converge to a Local Nash Equilibrium. arXiv:1706.08500 [cs.LG]
- [11] J. L. Hodges. 1958. The significance probability of the smirnov two-sample test. Arkiv för Matematik 3, 5 (1958), 469 – 486. https://doi.org/10.1007/BF02589501
- [12] Seung Wook Kim, Yuhao Zhou, Jonah Philion, Antonio Torralba, and Sanja Fidler. 2020. Learning to Simulate Dynamic Environments with GameGAN. arXiv e-prints, Article arXiv:2005.12126 (May 2020), arXiv:2005.12126 pages. arXiv:2005.12126 [cs.CV]
- [13] Adriano Koshiyama, Nick Firoozye, and Philip Treleaven. 2019. Generative Adversarial Networks for Financial Trading Strategies Fine-Tuning and Combination. arXiv e-prints, Article arXiv:1901.01751 (Jan. 2019), arXiv:1901.01751 pages. arXiv:1901.01751 [cs.LG]
- [14] J. McGinn, C. Messenger, M. J. Williams, and I. S. Heng. 2021. Generalised gravitational wave burst generation with generative adversarial networks. Classical and Quantum Gravity 38, 15, Article 155005 (Aug. 2021), 15500 pages. https://doi.org/10.1088/1361-6382/ac09cc arXiv:2103.01641 [astro-ph.IM]
- [15] Mehdi Mirza and Simon Osindero. 2014. Conditional Generative Adversarial Nets. arXiv e-prints, Article arXiv:1411.1784 (Nov. 2014), arXiv:1411.1784 pages. arXiv:1411.1784 [cs.LG]
- [16] Takeru Miyato, Toshiki Kataoka, Masanori Koyama, and Yuichi Yoshida. 2018. Spectral Normalization for Generative Adversarial Networks. arXiv e-prints, Article arXiv:1802.05957 (Feb. 2018), arXiv:1802.05957 pages. arXiv:1802.05957 [cs.LG]
- [17] Dhruv Patel and Assad A Oberai. 2019. Bayesian Inference with Generative Adversarial Network Priors. arXiv e-prints, Article arXiv:1907.09987 (July 2019), arXiv:1907.09987 pages. arXiv:1907.09987 [stat.ML]
- [18] Tim Salimans, Ian Goodfellow, Wojciech Zaremba, Vicki Cheung, Alec Radford, and Xi Chen. 2016. Improved Techniques for Training GANs. arXiv:1606.03498 [cs.LG]
- [19] Shuntaro Takahashi, Yu Chen, and Kumiko Tanaka-Ishii. 2019. Modeling financial time-series with generative adversarial networks. *Physica A: Statistical Mechanics* and its Applications 527 (2019), 121261. https://doi.org/10.1016/j.physa.2019. 121261
- [20] Aaron van den Oord, Sander Dieleman, Heiga Zen, Karen Simonyan, Oriol Vinyals, Alex Graves, Nal Kalchbrenner, Andrew Senior, and Koray Kavukcuoglu. 2016. WaveNet: A Generative Model for Raw Audio. arXiv e-prints, Article arXiv:1609.03499 (Sept. 2016), arXiv:1609.03499 pages. arXiv:1609.03499 [cs.SD]
- [21] Zhengwei Wang, Graham Healy, Alan F. Smeaton, and Tomás E. Ward. 2019. Use of Neural Signals to Evaluate the Quality of Generative Adversarial Network Performance in Facial Image Generation. Cognitive Computation 12, 1 (Aug 2019), 13–24. https://doi.org/10.1007/s12559-019-09670-y
- [22] Magnus Wiese, Robert Knobloch, Ralf Korn, and Peter Kretschmer. 2019. Quant GANs: Deep Generation of Financial Time Series. arXiv e-prints, Article arXiv:1907.06673 (July 2019), arXiv:1907.06673 pages. arXiv:1907.06673 [q-fin.MF]
- [23] Jinsung Yoon, Daniel Jarrett, and Mihaela van der Schaar. 2019. Time-series Generative Adversarial Networks. In Advances in Neural Information Processing Systems, H. Wallach, H. Larochelle, A. Beygelzimer, F. d'Alché-Buc, E. Fox, and R. Garnett (Eds.), Vol. 32. Curran Associates, Inc. https://proceedings.neurips.cc/ paper/2019/file/c9efe5f26cd17ba6216bbe2a7d26d490-Paper.pdf

- [24] Yuichi Yoshida and Takeru Miyato. 2017. Spectral Norm Regularization for Improving the Generalizability of Deep Learning. arXiv e-prints, Article arXiv:1705.10941 (May 2017), arXiv:1705.10941 pages. arXiv:1705.10941 [stat.ML]
- [25] Kang Zhang, Guoqiang Zhong, Junyu Dong, Shengke Wang, and Yong Wang. 2019. Stock Market Prediction Based on Generative Adversarial Network. Procedia Computer Science 147 (2019), 400–406. https://doi.org/10.1016/j.procs.2019.01.256 2018 International Conference on Identification, Information and Knowledge in the Internet of Things.

A UNBIASED ESTIMATORS FOR THE BINNED INSTRUMENT-SPECIFIC FEATURE DISTRIBUTIONS

Borrowing the notation from Sec. 3, we want to prove that the quantity $\hat{\mathbb{B}}_{c}^{[-,+]}$ in Eq. (6) is an unbiased estimator for the true binned marginal distribution $\mathbb{B}_{c}^{[-,+]}$ in Eq. (7).

Starting from Eq.(7)

$$\mathbb{B}_{c}^{[-,+]} \equiv \int_{-}^{+} d\Delta i_{c} \,\mathcal{F}\left(\Delta s; I_{t}\right) \tag{12}$$

$$= \int_{-}^{+} d\Delta i_{c} \,\int_{\mathbb{R}^{n^{i}}} d\Delta s \,\mathcal{P}_{m} \left(\Delta i_{c}; \hat{\boldsymbol{a}}, \Delta s\right) \mathcal{F}\left(\Delta s; I_{t}\right) \tag{13}$$

$$= \int_{\mathbb{R}^{n^{i}}} d\Delta s \,\int_{\mathbb{R}} d\Delta i_{c} \,\Theta_{-}^{+}(\Delta i_{c}) \mathcal{P}_{m} \left(\Delta i_{c}; \hat{\boldsymbol{a}}, \Delta s\right) \mathcal{P}_{I}^{p} \left(\Delta s\right) \tag{14}$$

$$= \int_{\mathbb{R}^{n}} d\Delta s \,\int_{\mathbb{R}} d\Delta i_{c} \,\Theta_{-}^{+}(\Delta i_{c}) \mathcal{P}_{m} \left(\Delta i_{c}; \hat{\boldsymbol{a}}, \Delta s\right) \right] \tag{15}$$

$$= \lim_{S_{t} \to \infty} \frac{1}{S_{t}} \times \tag{16}$$

$$= \lim_{S_{t} \to \infty} \frac{1}{S_{t}} \times \tag{16}$$

$$= \lim_{S_{t} \to \infty} \frac{1}{S_{t}} \times \tag{17}$$

$$= \lim_{S_{t} \to \infty} \frac{1}{S_{t}} \times \left[\Theta_{-}^{+}(\Delta i_{c}) \mathcal{P}_{m} \left(\Delta i_{c}; \hat{\boldsymbol{a}}, \Delta s_{j_{s}} \right) \right] \Big|_{\Delta s_{j_{s}}} \mathcal{S}_{\mathcal{F}}(\Delta s; I_{t})$$

$$= \lim_{S_{t} \to \infty} \frac{1}{I_{t} \times S_{t}} \sum_{j_{s}=1}^{S_{t}} \sum_{j_{i}=1}^{I} \left[\Theta_{-}^{+}(\Delta i_{j_{i}, c}) \right|_{\Delta i_{j_{i}=1, c}} \mathcal{S}_{\mathcal{F}}(\Delta s; I_{t})$$

$$= \lim_{S_{t} \to \infty} \frac{1}{I_{t} \times S_{t}} \sum_{j_{s}=1}^{S_{t}} \sum_{j_{i}=1}^{I} \left[\Theta_{-}^{+}(\Delta i_{j_{i}, c}) \right|_{\Delta i_{j_{i}=1, c}} \mathcal{S}_{\mathcal{F}}(\Delta s; I_{t})$$

$$\Delta i_{j_{i}=1, c} \mathcal{S}_{\mathcal{F}}(\Delta s; \hat{\boldsymbol{a}}, \Delta s_{j_{s}}) \tag{12}$$

Step by step: in Eq. (13) we used the law of total probability, in Eq. (14) we expanded the first integration domain to R such that it is possible to use its Monte Carlo Estimator in Eq. (15). In Eq. (17) we commute sum and integration operators thanks to the Fubini-Tonelli theorem and we finally rely on the Monte Carlo Estimator for the integration over Δi_c . Please note that it is possible for us to compute the Monte Carlo Estimators needed as the samples $\Delta s \sim \mathcal{P}_I^p \left(\Delta s\right)$ and $\Delta i_c \sim \mathcal{P}_m \left(\Delta i_c; \hat{\boldsymbol{a}}, \Delta s_{j_s}\right)$ are respectively drawn by the trained generator $\boldsymbol{\mathcal{S}}$ and $\boldsymbol{\mathcal{I}}$.

B GAN FRAMEWORK

 $=\lim_{N_t\to\infty}\hat{\mathbb{B}}_c^{\left[-,+\right]}$

In this framework a generator and a discriminator are trained together in a zero-sum game (if one wins, the other loses) to reach the optimal solution where the model has learnt characteristics of input data and is able to generate new realistic samples indistinguishable from the real ones.

To model generator's distribution p_g over training data p_{data} we define an input noise variable $\mathbf{z} \sim p(\mathbf{z})$ also called latent space and then represent a mapping from this latent space to data space as $G(\mathbf{z})$ with G being a differentiable function represented by a multilayer perceptron. Then we have D a second multilayer perceptron that outputs a scalar $D(\mathbf{x})$ which stands for the probability that \mathbf{x} comes from p_{data} rather than p_g . D is then trained to maximize the probability of assigning the correct labels to both synthetic and real samples, while G is trained to maximize the classification error of D. From a theoretical perspective G and D are playing the following minimax game :

$$\min_{G} \max_{D} V(D, G) = \mathbb{E}_{\mathbf{x} \sim p_{data(\mathbf{x})}} [\log D(\mathbf{x})] + \mathbb{E}_{\mathbf{z} \sim p_{\mathbf{z}}} [\log (1 - D(G(\mathbf{z})))]$$
(20)

The optimal training case also called Nash Equilibrium is reached when the generator perfectly reproduces real data and the discriminator can no longer distinguish real and fake samples. In any cases $D(\mathbf{x})$ outputs a probability of 50%.

$$D^*(\mathbf{x}) = \frac{p_{data}(\mathbf{x})}{p_{data}(\mathbf{x}) + p_g(\mathbf{x})} = \frac{1}{2}$$
 (21)

with $p_g = p_{data}$.

(19)

Generative adversarial networks are known to be difficult to train due to several unstabilities, discriminator and generator must be synchronized during training, in order to avoid "mode collapse" phenomenon, a scenario where G, which has been trained too much in comparison of D, collapses too many values from \mathbf{z} to the same value of \mathbf{x} to maintain acceptable diversity to model p_{data} .

Another common issue happens during early training phase, when G is still producing poor generated samples, D task is easy and generated samples are easily identified as fake samples. In that situation D provides no reliable gradient informations leading to a vanishing gradients situation.

B.1 Wasserstein GAN

Introduced in 2017, by Arjovsky et al. [1], Wasserstein GANs empirically showed they were able to cure the main training issues faced by Vanilla GANs. Training a WGAN no longer requires to maintain a fragile balance between the discriminator and the generator nor an expansive redesign of networks architecture. Mode collapse scenarios are reduced and loss curves correlate to observed samples quality. To achieve such properties WGANs minimize a reasonable and efficient approximation of the Earth Mover distance W(q,p), also called Wasserstein-1.

$$\min_{G} \max_{D} V(D, G) = \mathbb{E}_{\mathbf{x} \sim p_{data(\mathbf{x})}} [D(\mathbf{x})] - \mathbb{E}_{\mathbf{z} \sim p_{\mathbf{z}}} [D(G(\mathbf{z}))] \quad (22)$$

This distance is defined as the minimum cost of transporting mass in order to transform a distribution q into a distribution p.

W(q,p) being considered as continuous and differentiable almost everywhere a Lipschitz constraint is also enforced at discriminator level, to assure informative gradients that can later be used for the generator thus making its optimization easier and providing a better behavior than its Vanilla GANs counterpart. Standard WGANs are using clipping to force discriminator weights to lie within a compact space [-c, c], Gulrajani et al. [9] showed limitations and issues with

this method and proposed a better way of enforcing a Lipschitz constraint with a technique called gradient penalty. The objective function becomes

$$\min_{G} \max_{D} V(D, G) = \mathbb{E}_{\mathbf{z} \sim p_{\mathbf{z}}} [D(G(\mathbf{z}))] - \mathbb{E}_{\mathbf{x} \sim p_{data}(\mathbf{x})} [D(\mathbf{x})] + \lambda \mathcal{L}_{P}$$
(23)

where \mathcal{L}_P is the gradient penalty term defined by

$$\mathcal{L}_P = \mathbb{E}_{\hat{\mathbf{x}} \sim p_{\hat{\mathbf{x}}}} [(\|\nabla_{\hat{\mathbf{x}}_i} D(\hat{\mathbf{x}})\|_2 - 1)^2]$$
 (24)

and $\hat{\mathbf{x}}$ a new distribution crafted from data distribution p_{data} and generator distribution p_g

$$\hat{\mathbf{x}} = \epsilon \ \mathbf{x} + (1 - \epsilon) \ G(\mathbf{z}) \tag{25}$$

The only drawbacks of this method is a strong dependence on the current generative distribution at a given time step and an increased computational cost due to the gradient penalty term which requires a new forward and backward pass propagation, as stated in [16].

B.2 BiGANs

BiGAN is a type of GAN where the generator not only maps latent samples generated data, but also has an inverse mapping from the data to the latent representation [6]. In addition to the usual G and D networks, BiGAN includes an additional encoder network E that learns to map $\mathbf x$ data to $\mathbf z$ latent representations, hence forming a coupled system $\{G, E\}$. The discriminator is also slightly modified to discriminate jointly in data/latent space $(\mathbf x, E(\mathbf x))$ vs $(G(\mathbf z), \mathbf z)$, where the latent component is either an output of the encoder $E(\mathbf x)$ or an input of the generator $G(\mathbf z)$ (Fig. 2). The discriminator $D(\mathbf x, \mathbf z)$ is then normally trained to discern whether the couple $(\mathbf x, \mathbf z)$ comes from a real or generated data distribution.

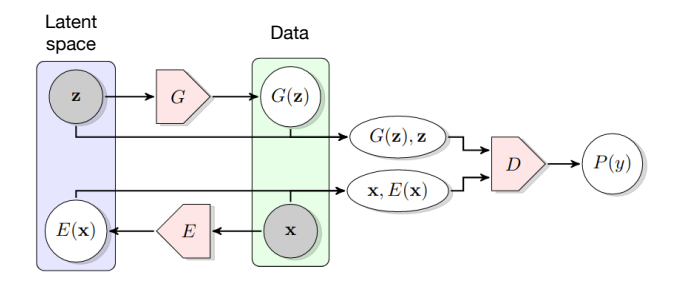


Figure 2: The structure of Bidirectional Generative Adversarial Networks (BiGAN) (Source: [6]).

In this setup fooling D finally leads G and E to minimize the differences between $(G(\mathbf{z}), \mathbf{z})$ and $(\mathbf{x}, E(\mathbf{x}))$ couples.

$$\min_{G,E} \max_{D} V(D, E, G) = \mathbb{E}_{\mathbf{x} \sim p_{data(\mathbf{x})}} \left[\log D(\mathbf{x}, E(\mathbf{x})) \right] + \mathbb{E}_{\mathbf{z} \sim p_{\mathbf{z}}} \left[\log (1 - D(G(\mathbf{z}), \mathbf{z})) \right]$$
(26)

Although BiGAN is a robust and highly generic approach to unsupervised feature learning, making no assumptions about data type nor structure, as shown in [6], they still suffer from a lack of constraints on E and G being aligned (i.e. $E^{-1} = G$ and $G^{-1} = E$ are not guaranteed). In a data space exploration scenario (using latent

as prior) this can lead to errors because of the reconstructed latent being out-of-distribution. To solve this issue, the authors from [4] introduced a cycle consistency regularization term \mathcal{L}_C to both E and G to promote alignment and defined as follow

$$\mathcal{L}_C(\mathbf{x}, \mathbf{z}) = \mathcal{L}_R(\mathbf{x}) + \mathcal{L}_{R'}(\mathbf{z})$$
 (27)

where

$$\mathcal{L}_R(\mathbf{x}) = \|\mathbf{x} - G(E(\mathbf{x}))\|_1 \tag{28}$$

$$\mathcal{L}_{R'}(\mathbf{z}) = \|\mathbf{z} - E(G(\mathbf{z}))\|_{1}$$
(29)

The new loss for E and G become a linear combination between the selected generator/encoder loss and \mathcal{L}_C

$$\mathcal{L}^*_{E,G} = (1 - \alpha)\mathcal{L}_{E,G} + \alpha\mathcal{L}_C \tag{30}$$